

# CdSe–ZnS Quantum Dots as Resonance Energy Transfer Donors in a Model Protein–Protein Binding Assay

Dale M. Willard,<sup>†</sup> Lori L. Carillo, Jaemyeong Jung, and Alan Van Orden\*

*Department of Chemistry, Colorado State University, Fort Collins, Colorado 80523*

Received June 13, 2001; Revised Manuscript Received July 10, 2001

## ABSTRACT

Specific binding of biotinylated bovine serum albumin (bBSA) and tetramethylrhodamine-labeled streptavidin (SAV–TMR) was observed by conjugating bBSA to CdSe–ZnS core–shell quantum dots (QDs) and observing enhanced TMR fluorescence caused by fluorescence resonance energy transfer (FRET) from the QD donors to the TMR acceptors. Because of the broad absorption spectrum of the QDs, efficient donor excitation could occur at a wavelength that was well resolved from the absorption spectrum of the acceptor, thereby minimizing direct acceptor excitation. Appreciable overlap of the donor emission and acceptor absorption spectra was achieved by size-tuning the QD emission spectrum into resonance with the acceptor absorption spectrum, and cross-talk between the donor and acceptor emission was minimized because of the narrow, symmetrically shaped QD emission spectrum. Evidence for an additional, nonspecific QD–TMR energy transfer mechanism that caused quenching of the QD emission without a corresponding TMR fluorescence enhancement was also observed.

Fluorescence resonance energy transfer (FRET) is a process whereby the electronic excitation energy of a donor chromophore is nonradiatively transferred to a nearby acceptor molecule via a through-space dipole–dipole interaction between the donor–acceptor pair.<sup>1–5</sup> FRET occurs when there is appreciable overlap between the emission spectrum of the donor and the absorption spectrum of the acceptor. The strong distance dependence of the FRET efficiency has been widely exploited in studying the structure and dynamics of proteins and nucleic acids, in the detection and visualization of intermolecular association, and in the development of intermolecular binding assays.<sup>6</sup> FRET-based studies involving pairs of organic dye molecules as the donor–acceptor complexes are often limited by cross-talk caused by spectral overlap of the donor and acceptor emission. The need for significant overlap between the emission and absorption spectra of the donor and acceptor, coupled with the narrow absorption spectrum of conventional organic dye molecules, makes it difficult to avoid direct excitation of the acceptor molecules at the excitation wavelength needed to efficiently excite the donor. In addition, the broad emission spectrum of the donor, with its long red tail, can often overlap significantly with the emission spectrum of the acceptor. Several recent reports have confirmed that luminescent semiconductor quantum dots (QDs), such as CdSe and CdTe, are able to participate in resonance energy transfer processes analogous to FRET,<sup>7–10</sup> which makes these materials good

candidates to overcome some of the limitations associated with conventional organic dye molecules in FRET-based studies of biomolecular structure, ligand–receptor binding, etc.

Semiconductor QDs are currently being investigated for their use as luminescent biological probes because of their high photostability relative to organic dye molecules and their unique, size tunable spectral properties.<sup>11–14</sup> QDs possessing high luminescence quantum yields under ambient conditions (i.e., CdSe–ZnS core–shell QDs) are normally used for such applications, enabling the use of ultrasensitive detection methods with sensitivity down to the single molecule limit. Our goal is to exploit the unique spectral properties of these materials in the design of FRET-based studies that can overcome some of the problems encountered when pairs of organic dye molecules are used as the donor–acceptor complexes. Initially, we plan to develop ligand–receptor assays in the solution phase, wherein intermolecular binding is observed via FRET between a QD donor attached to one of the binding partners and an organic acceptor dye attached to the other partner. Our motivation for doing this is severalfold. (1) Because of the broad absorption spectra of semiconductor QDs, there is great flexibility in the selection of the donor excitation wavelength. Efficient excitation of the donor can thus occur at a wavelength where direct excitation of the acceptor is minimal, which will reduce cross-talk between the donor and acceptor emission spectra. (2) Binding assays can be designed in which there is an extremely large red shift of the acceptor emission spectrum relative to the excitation wavelength of the donor. This will

\* Corresponding author. E-mail: vanorden@lamar.colostate.edu.

<sup>†</sup> Present address: Institut für Physikalische und Theor. Chemie, Universität Tübingen, 72076 Tübingen, Germany.

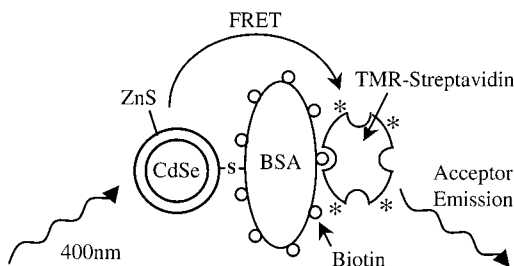


**Figure 1.** Schematic of the FRET binding assay. For clarity, only one protein complex is shown.

potentially enable higher sensitivity detection in complex media, such as blood or tissue, than would be possible via conventional FRET. Most of the background interference in such media is caused by scattered light and autofluorescence, which mainly occurs near the excitation wavelength and will thus be well resolved from the acceptor emission. By monitoring only the enhanced fluorescence of the acceptor, we anticipate that it will be possible to detect ligand–receptor binding in homogeneous assays with greater sensitivity and simplicity than conventional assays that are used to perform chemical analysis in such media. (3) Semiconductor QDs possess narrower emission spectra than conventional organic dye molecules, and their emission spectra do not tail-off to the red, which minimizes the spectral overlap of the donor and acceptor emission spectra and further reduces cross talk. (4) The emission spectra of semiconductor QDs are readily size tunable. This will enable tuning the emission spectrum of the acceptor to enhance the energy transfer efficiency and optimizing the spectral resolution of the donor and acceptor emission. By varying the size and/or composition of the material, semiconductor QDs can be prepared with emission spectra at any visible wavelength, which will enable the custom synthesis of an efficient energy transfer donor for any visible absorbing chromophore.

This letter presents the first step toward accomplishing the goals outlined above. We demonstrate a biotin–streptavidin binding assay wherein specific binding of tetramethylrhodamine-labeled streptavidin (SAv–TMR, 4:1:1 TMR:SAv ratio, Molecular Probes) to biotinylated bovine serum albumin (bBSA, 9:1 biotin:BSA ratio, Sigma) conjugated to CdSe–ZnS core–shell QDs (QD–bBSA) is observed via enhancement of the TMR fluorescence due to QD–TMR FRET (Figure 1). Preparation of the binding assay involved synthesis of CdSe–ZnS core–shell QDs, extraction of the QDs into aqueous solution, conjugating the QDs to bBSA, and reacting the QD–bBSA complexes with varying concentrations of SAv–TMR. Trioctylphosphine/trioctylphosphine oxide (TOP/TOPO) capped CdSe–ZnS QDs with a core diameter of 3.1 nm were prepared in our laboratory using established synthetic methods.<sup>15–17</sup> The core diameters were determined from the correspondence of the absorption spectrum with the particle diameter.<sup>15</sup> QD solution concentrations were estimated from the absorption spectra using the molar absorptivity at the first absorption maximum for QDs of this size reported by Schmelz et al. ( $\sim 1 \times 10^5 \text{ M}^{-1} \text{ cm}^{-1}$ ).<sup>18</sup> A luminescence quantum yield of  $\sim 40\%$  was

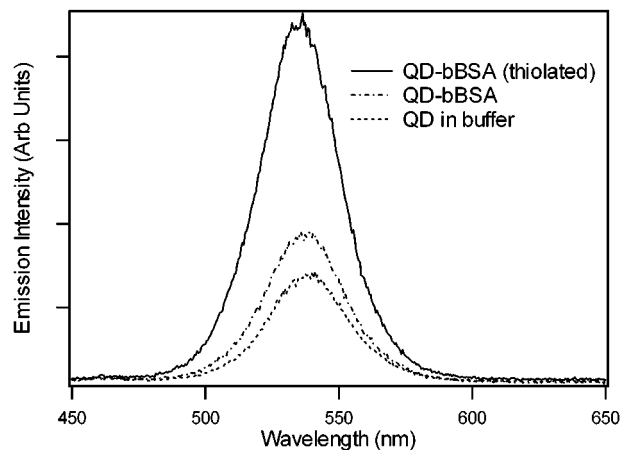


**Figure 2.** Emission spectra observed from  $\sim 15 \text{ nM}$  mercaptoacetic acid-capped CdSe–ZnS QDs,  $\sim 15 \text{ nM}/\sim 70 \text{ nM}$  QDs/unthiolated bBSA, and  $\sim 15 \text{ nM}/\sim 70 \text{ nM}$  QDs/thiolated bBSA. All solutions were prepared in 1 mM PBS buffer (pH 8). The excitation wavelength was 400 nm.

measured for these QDs by comparison with the fluorescence emission of Rhodamine 6G (R6G).<sup>19</sup>

Water soluble QDs were prepared by diluting  $\sim 100 \mu\text{L}$  of  $\sim 1 \text{ mM}$  TOP/TOPO-capped QD/hexane solution in  $\sim 1 \text{ mL}$  of *n*-butanol; precipitating the QDs by addition of methanol; centrifuging, washing, and redissolving the precipitate in  $\sim 2 \text{ mL}$  of chloroform; and then reacting the QDs with  $\sim 150 \mu\text{L}$  of mercaptoacetic acid for at least 2 h. Exchange of the TOP/TOPO capping groups with mercaptoacetic acid caused the QDs to precipitate out of the solution. The resulting precipitate was centrifuged, washed, suspended in  $\sim 2 \text{ mL}$  of 1 mM phosphate buffered saline solution (PBS, pH 8) and then dissolved by dropwise addition of concentrated NaOH. After the QDs were reprecipitated with acetone, centrifuged, and washed, they were able to dissolve in PBS buffer. The mercaptoacetic acid capped QDs were stable in aqueous buffer for up to 3 days, after which the QDs precipitated out of solution. Preparation of the QD–bBSA complex was accomplished by, first, treating the bBSA with 2-iminothiolane in PBS buffer to introduce sulfhydryl residues onto the proteins at a sulfhydryl:protein ratio of  $\sim 20:1$ .<sup>20</sup> The favorable interaction between the thiol groups attached to the proteins and the QD surface enhanced the binding affinity of the QD–protein complex in a manner similar to that described by Mitchell et al. in the reaction of thiol-terminated DNA with mercaptopropionic acid-capped CdSe–ZnS QDs.<sup>21</sup> Evidence for this comes from the large enhancement of the QD luminescence observed following the reaction with thiolated bBSA compared to the uncomplexed QDs in aqueous solution (Figure 2). Dissolving the QDs in buffer resulted in a  $\sim 4$ -fold reduction in the luminescence quantum yield relative to that observed for the TOP/TOPO-capped QDs in organic solvent. The quantum yield returned to its original value of  $\sim 40\%$  after formation of the QD–bBSA complex. By contrast, reaction of QDs with unthiolated bBSA resulted in a much smaller enhancement in the quantum yield (Figure 2), possibly due to nonspecific adsorption of the bBSA molecules to the QD surface. Such enhancements in the QD luminescence upon formation of

QD–protein conjugates have been observed previously and attributed to alteration of the environment polarity of the CdSe core due to surface charge neutralization.<sup>13</sup> Once formed, the QD–bBSA conjugates were stable in solution for a period of several weeks, although all of the experiments described herein were carried out within 2–3 days of formation of the conjugates.

The concentrations of QD and bBSA in the reaction mixture were determined by UV/vis spectrophotometry to be  $\sim 2$  and  $\sim 70 \mu\text{M}$ , respectively,<sup>22</sup> implying an excess of unconjugated bBSA. We were able to lower the concentration of unconjugated bBSA by filtration through a 100 kD molecular weight cutoff spin column (Micron YM-100, Millipore Corp.). Unbound bBSA ( $M_w$  68 kD) was detected in the solution that passed through this column, but QDs were not, which suggests that most of the QDs in this sample were conjugated to at least two bBSA molecules. Further attempts to lower the bBSA concentration by this filtration method were unsuccessful, most likely due to the presence of unconjugated bBSA complexes that were too large to pass through the spin column. After diluting the solution that remained on the column to 1 mL, the final QD and bBSA concentrations were found to be  $\sim 2$  and  $\sim 30 \mu\text{M}$ , respectively. At this time, we are unable to determine the exact stoichiometry of the QD–bBSA complexes formed. A rough calculation of the maximum number of bBSA molecules that could be packed around a spherical QD of this size gives  $\sim 11$  bBSA molecules per QD,<sup>23</sup> which indicates that at least a third of the bBSA molecules still present were unconjugated. For the purposes of this calculation, bBSA was considered to be a hard sphere of radius 50 Å. BSA is actually an ellipsoidal-shaped molecule with unit cell dimensions of  $60 \times 60 \times 100 \text{ Å}^3$ ,<sup>24</sup> which subjects this calculation to error. It is most likely the case that there is a distribution of QD–bBSA complexes, and so an even larger excess of unconjugated bBSA cannot be ruled out. We also cannot rule out the presence of QD–bBSA complexes that contain more than one QD, although extensive aggregation of the QDs would be inconsistent with the observed enhancement of the QD luminescence upon formation of the complexes. As will become apparent below, the uncertainties noted here do not materially detract from the main objective of this report, which is to demonstrate QD–dye FRET due to a specific biomolecular interaction.

Figure 3 displays absorption and emission spectra obtained from pure solutions of the QD–bBSA and SAV–TMR samples used in these experiments. The QD size was chosen so as to maximize the spectral overlap of the donor–acceptor emission and absorption spectra while still maintaining good spectral resolution of the donor and acceptor emission. The FRET efficiency of a donor–acceptor pair is characterized by the Förster radius,  $R_0$ , which is defined as the donor–acceptor distance corresponding to 50% efficiency. Calculation of the donor–acceptor emission–absorption spectral overlap, and knowledge of the photophysical properties of the QDs and TMR molecules, lead to an  $R_0$  value of 54 Å for this donor–acceptor pair.<sup>25</sup> This is comparable to the highest  $R_0$  values obtained for the most commonly used

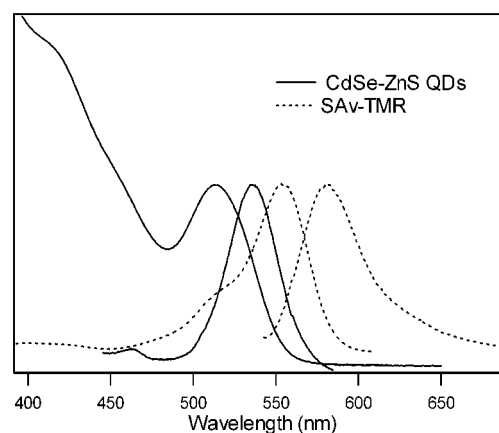


**Figure 3.** Normalized absorption and emission spectra observed from pure solutions of CdSe–ZnS QDs conjugated to bBSA and SAV–TMR. Solutions were prepared in 1 mM PBS buffer. The QD absorption spectrum is consistent with a CdSe core diameter of 3.1 nm, and the fwhm spectral width of the QD emission (35 nm) is indicative of a  $\sim 10\%$  size distribution.

organic dye pairs in FRET applications.<sup>3,4</sup> For example,  $R_0$  values for the widely used fluorescein–TMR pair are normally reported to be in the range 49–55 Å.<sup>3,4</sup> We anticipate that it will be possible to further enhance the FRET efficiencies in such QD–dye systems by fine-tuning the size, size distribution, and luminescence quantum yields of the QDs and/or by choosing donor dyes with larger absorption cross sections and/or Stokes shifts.

Binding assays were prepared by reacting 15  $\mu\text{L}$  aliquots of QD–bBSA in PBS buffer with 2–20  $\mu\text{L}$  of 16  $\mu\text{M}$  SAV–TMR in pH 8 buffer. After  $\sim 5$ -min of incubation time, the reaction mixtures were diluted to 2 mL in PBS buffer, and the resulting solutions were placed in 1 cm path length quartz cuvettes. The final concentrations of the QD–bBSA and SAV–TMR were  $\sim 15$  nM and 16–160 nM, respectively. Figure 4 displays the emission spectra observed for these samples. Emission spectra obtained from pure solutions of  $\sim 15$  nM QD–bBSA and 160 nM SAV–TMR are also shown for comparison. An excitation wavelength of 400 nm was used for all samples. At this wavelength, QD excitation occurs with high efficiency, while direct TMR excitation is minimal (see Figure 3). The strong enhancement in the TMR fluorescence observed for the QD–bBSA/SAV–TMR solutions is consistent with QD–TMR FRET due to specific binding of SAV–TMR and QD–bBSA. To confirm this, we repeated the assay using QD bioconjugates formed from nonbiotinylated BSA (QD–BSA). Figure 5 displays the emission spectrum observed from a sample containing  $\sim 15$  nM QD–BSA and 120 nM SAV–TMR. Also shown are the spectra from pure solutions of  $\sim 15$  nM QD–BSA and 120 nM SAV–TMR and an “extracted” SAV–TMR spectrum. The latter was obtained by fitting the region of the QD emission to a pure QD spectrum and then subtracting the fitted spectrum from the entire QD–BSA/SAV–TMR spectrum. Comparison of the extracted spectrum with that of the 120 nM SAV–TMR solution revealed that  $\sim 90\%$  of the emission observed in the spectral region corresponding to TMR fluorescence is due to direct excitation of TMR. The

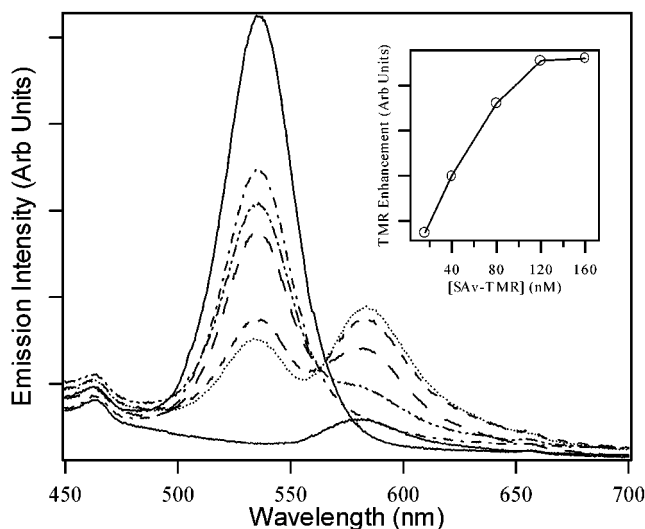


**Figure 4.** Fluorescence emission spectra from solutions containing  $\sim 15$  nM QD-bBSA and 0 (—), 16 (— · —), 40 (— · · —), 80 (— · · · —), 120 (— · · · · —), and 160 nM (····) SAV-TMR. The lower solid curve is from a 160 nM SAV-TMR control. All solutions were prepared in 1 mM PBS buffer. An excitation wavelength of 400 nm was used for all samples. The inset displays the enhanced TMR fluorescence intensity at 585 nm from the QD-bBSA/SAV-TMR solutions as a function of SAV-TMR concentration. The enhanced fluorescence intensities were obtained by extracting the TMR fluorescence spectrum from each spectrum and correcting for background and direct TMR excitation as described in the text.

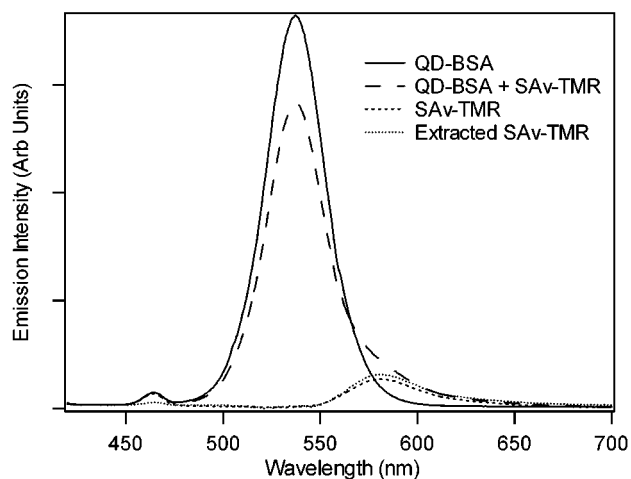


**Figure 5.** Emission spectra observed from  $\sim 15$  nM QD-bBSA,  $\sim 15$  nM/120-nM QD-bBSA/SAV-TMR, and 120 nM SAV-TMR solutions in 1 mM PBS buffer. An extracted SAV-TMR spectrum is also shown for comparison. The excitation wavelength was 400 nm.

$\sim 10\%$  enhancement in the TMR fluorescence is possibly due to QD-TMR FRET caused by a small amount of nonspecific adsorption of SAV-TMR molecules onto the QDs. However, this should be compared to the 4-fold enhancement in the TMR fluorescence observed for the  $\sim 15$  nM/120 nM QD-bBSA/SAV-TMR solution, which confirms that the enhanced fluorescence in this solution is due to QD-TMR FRET caused predominantly by specific biotin-SAV binding. The enhanced TMR fluorescence, obtained by extracting the SAV-TMR spectra as described above and correcting for direct TMR excitation and back-

**Table 1.** Fraction of FRET-Induced QD Emission Quenching vs SAV-TMR Concentration

[SAV-TMR] (nM)	16	40	80	120	160
$f(\%)$	11	30	54	46	47

ground contributions, is plotted as a function of the SAV-TMR concentration in the inset to Figure 4. Since we are interested in designing binding assays that monitor the enhanced fluorescence of the acceptor, the sharp rise in the enhanced TMR fluorescence with concentration is encouraging. However, it should be noted that, at present, we are unable to predict the binding affinity of the complexes from these data because the exact stoichiometry of the QD-bBSA conjugates and their complexes with SAV-TMR are not known.

Although QD-TMR FRET is clearly responsible for the enhanced TMR fluorescence in these assays, it is apparent from the concentration dependence of the QD emission that other types of energy transfer mechanisms, in addition to FRET, need to be considered as contributing factors in the quenching of the QD emission. The fraction,  $f$ , of the QD emission that is quenched due to QD-TMR FRET is given by<sup>6</sup>

$$f = \frac{\Delta I_{\text{FRET}}^{\text{TMR}} \cdot \phi_{\text{L}}^{\text{QD}}}{\Delta I_{\text{quench}}^{\text{QD}} \cdot \phi_{\text{F}}^{\text{TMR}}} \quad (1)$$

where  $\Delta I_{\text{FRET}}^{\text{TMR}}$  is the enhanced TMR fluorescence,  $\Delta I_{\text{quench}}^{\text{QD}}$  is the difference in the QD emission intensities in the absence and presence of SAV-TMR, and  $\phi_{\text{F}}^{\text{TMR}}$  and  $\phi_{\text{L}}^{\text{QD}}$  are the luminescence quantum efficiencies of the SAV-TMR (0.27, measured with reference to R6G) and QDs (0.4) in the absence of the donor and acceptor, respectively. The  $f$  values calculated at each SAV-TMR concentration are presented in Table 1. For the 16 nM SAV-TMR solution, the fraction of the QD emission quenched due to FRET is only 11%, indicating that 89% of the donor quenching is initially being caused by another energy transfer mechanism that does not enhance the TMR fluorescence. The value of  $f$  increases to a maximum of 54% as the SAV-TMR concentration increases to 80 nM and then levels off at 46% for concentrations of 120 nM and above. Clearly, the largest fraction of static quenching not resulting in enhanced TMR fluorescence occurs upon addition of 16 nM SAV-TMR. Most of the QD emission quenching observed upon increasing the SAV-TMR concentration beyond this amount can be attributed to QD-TMR FRET. For example, comparison of the QD quenching and enhanced TMR fluorescence of the 16 and 40 nM SAV-TMR samples reveals that QD-TMR FRET is responsible for 88% of the difference between the QD emission intensities of these two samples.

Alternative energy transfer mechanisms that could possibly account for the additional quenching of the QD emission include QD self-quenching caused by the formation of QD aggregates due to binding of multiple biotin moieties to a single SAV-TMR molecule and nonspecific interactions



between the TMR molecules and the QD surfaces, such as QD to TMR electron transfer. The following observations suggest that some type of nonspecific interaction between the QDs and TMR molecules is responsible for the large initial quenching observed in the 16 nM SAV–TMR solution. (1) A solution of ~15 nM QD–bBSA and 16 nM unlabeled SAV showed no measurable decrease in the QD emission, which indicates that QD aggregation is not significant at this SAV concentration and that the presence of TMR is crucial for this type of energy transfer to occur. (2) Note from Figure 5 that significant quenching of the QD emission is observed in a mixture of SAV–TMR and QDs conjugated to nonbiotinylated BSA even though there is no specific interaction between the QD–BSA complexes and SAV–TMR molecules. Previous studies have shown that electron and/or hole acceptor molecules, including organic dye molecules, in direct contact with the surfaces of CdSe and CdSe–ZnS QDs can quench the QD emission in a similar manner.<sup>18,26</sup> Thus, we speculate that QD to TMR electron transfer may be responsible for most of the initial quenching observed in the 16-nM SAV–TMR spectrum displayed in Figure 4. We further speculate that most of the QD surface sites available for nonspecific interaction with TMR are saturated at 16 nM SAV–TMR, which would explain why subsequent addition of SAV–TMR results mainly in QD–TMR FRET. Finally, we note that at higher SAV concentrations, we begin to see evidence for self-quenching of the QD emission due to QD aggregation. Each SAV–TMR molecule contains four biotin binding sites, and each bBSA molecule contains multiple biotin moieties, which means that at high SAV–TMR concentrations the potential exists for extensive cross-linking to occur. Our experiments with unlabeled SAV revealed evidence for self-quenching of the QD emission for solutions containing ~15 nM QD–bBSA and >80 nM SAV. For example, a solution containing ~15 nM QD–bBSA and 160 nM SAV caused the QD emission to decrease by 20% compared to the pure solution of ~15 nM QD–bBSA. The fact that the fraction of QD quenching caused by QD–TMR FRET reaches a peak at 80 nM SAV–TMR (See Table 1) may be due to the onset of QD self-quenching above this concentration.

In summary, we have shown that the specific binding of different proteins can be observed via FRET between a CdSe–ZnS QD donor attached to one of the proteins and organic acceptor dyes attached to the other protein, resulting in a strong enhancement of the dye fluorescence that was well resolved from the QD emission spectrum. Because of the broad absorption spectrum of the QDs, we were able to choose a donor excitation wavelength that was well resolved from the absorption spectrum of the acceptor, thereby minimizing direct excitation of the acceptor. Evidence for additional energy transfer processes that cause quenching of the QD emission without enhancing the dye fluorescence was also observed, the exact nature of which is the subject of continued investigation in our laboratory. The methods outlined in this report will be put to use in the design of homogeneous assays of antibody–antigen binding, DNA hybridization, enzyme–substrate interaction, etc.

**Acknowledgment.** Funding was provided by Colorado State University; the American Chemical Society, through a Petroleum Research Fund Type G Starter Grant to A.V.O., and Research Corporation, through a Research Innovation Award to A.V.O. L.L.C. is a McNair Undergraduate Scholar, and J.J. is the recipient of a 3F Graduate Fellowship from CSU. We thank Dr. Masaru Kuno (JILA and Naval Research Lab) for assisting us with the QD preparation, Dr. Steven Emory (Western Washington University) for suggesting the binding assay and for many helpful discussions, and Justin Benore for technical assistance.

## References

- (1) Stryer, L. *Annu. Rev. Biochem.* **1978**, *47*, 819–846.
- (2) Fairclough, R. H.; Cantor, C. H. *Methods Enzymol.* **1978**, *48*, 347–379.
- (3) Wu, P.; Brand, L. *Anal. Biochem.* **1994**, *218*, 1–13.
- (4) Van Der Meer, B. W.; Coker, G., III; Chen, S.-Y. S. *Resonance Energy Transfer: Theory and Data*; VCH: New York, 1994.
- (5) Selvin, P. R. *Methods Enzymol.* **1995**, *246*, 300–334.
- (6) Schobel, U.; Egelhaaf, H.-J.; Brecht, A.; Oelkrug, D.; Gauglitz, G. *Bioconjugate Chem.* **1999**, *10*, 1107–1114.
- (7) Kagan, C. R.; Murray, C. B.; Nirmal, M.; Bawendi, M. G. *Phys. Rev. Lett.* **1996**, *76*, 1517–1520.
- (8) Kagan, C. R.; Murray, C. B.; Bawendi, M. G. *Phys. Rev. B* **1996**, *54*, 8633–8643.
- (9) Finlayson, C. E.; Ginger, D. S.; Greenham, N. C. *Chem. Phys. Lett.* **2001**, *338*, 83–87.
- (10) Mamedova, N. N.; Kotov, N. A.; Rogach, A. L.; Studer, J. *Nano Lett.* **2001**, *1*, 281–286.
- (11) Bruchez, M., Jr.; Moronne, M.; Gin, P.; Weiss, S.; Alivisatos, A. P. *Science* **1998**, *281*, 2013–2016.
- (12) Chan, W. C. W.; Nie, S. *Science* **1998**, *281*, 2016–2018.
- (13) Mattoussi, H.; Mauro, J. M.; Goldman, E. R.; Anderson, G. P.; Sundar, V. C.; Mikulec, F. V.; Bawendi, M. G. *J. Am. Chem. Soc.* **2000**, *122*, 12142–12150.
- (14) Pathak, S.; Choi, S.-K.; Arnheim, N.; Thompson, M. E. *J. Am. Chem. Soc.* **2001**, *123*, 4103–4104.
- (15) Murray, C. B.; Norris, D. J.; Bawendi, M. G. *J. Am. Chem. Soc.* **1993**, *115*, 8706–8715.
- (16) Dabbousi, B. O.; Rodriguez-Viejo, J.; Mikulec, F. V.; Heine, J. R.; Mattoussi, H.; Ober, R.; Jensen, K. F.; Bawendi, M. G. *J. Phys. Chem. B* **1997**, *101*, 9463–9475.
- (17) Hines, M. A.; Guyot-Sionnest, P. *J. Phys. Chem.* **1996**, *100*, 468–471.
- (18) Schmelz, O.; Mews, A.; Basché, T.; Herrmann, A.; Müllen, K. *Langmuir* **2001**, *17*, 2861–2865.
- (19) Georges, J.; Arnaud, N.; Parise, L. *Appl. Spectrosc.* **1996**, *50*, 1505–1511.
- (20) A 5 mg sample of bBSA dissolved in 1 mL of PBS buffer was reacted with 2 mg of 2-iminothiolane·HCl (Sigma) and stored at 4 °C for 2 h with occasional vortex. The resulting solution was filtered through a size-exclusion centrifugal filter device (Micron YM-30, Millipore Corporation, Bedford, MA) and diluted to 1 mL in PBS buffer. 5,5'-Dithiobis(2-nitrobenzoic acid) (99%, Aldrich) was used to quantify the labeling degree of free thiol groups on the bBSA. A 4 mg amount of this reagent was reacted with 200  $\mu$ L of the bBSA solution, and the labeling degree was determined from absorbance measurements at 278 and 412 nm.
- (21) Mitchell, G. P.; Mirkin, C. A.; Letsinger, R. L. *J. Am. Chem. Soc.* **1999**, *121*, 8122–8123.
- (22) Molar absorptivities for bBSA and CdSe–ZnS at 278 nm of  $4.55 \times 10^4$  and  $\sim 6 \times 10^5$  M<sup>-1</sup> cm<sup>-1</sup>, respectively, were used to determine the concentrations by UV/vis spectrophotometry.
- (23)  $N = 0.65 [(R_2^3 - R_1^3)/R_p^3]$  (ref 13), where  $N$  is the maximum number of proteins that can be packed around a single QD,  $R_1$  is the radius of the core–shell QD ( $\sim 3$  nm) and  $R_2 \sim R_1 + 2R_p$ , where  $R_p$  is the radius of the protein ( $\sim 5$  nm).
- (24) Carter, D. C.; Ho, J. X. *Adv. Protein Chem.* **1994**, *45*, 153–203.
- (25)  $R_0 = (JK^2Q_Dn^{-4})^{1/2} \times 9.7 \times 10^3$  Å (ref 1), where  $K$  is the orientation factor,  $Q_D$  is the quantum yield of the unpaired donor,  $n$  is the solvent refractive index, and  $J$  is the overlap integral (M<sup>-1</sup> cm<sup>3</sup>), given by  $J$

$= f\epsilon_A(\lambda) f_D(\lambda)\lambda^4 d\lambda/f_D(\lambda) d\lambda$ , where  $\epsilon_A$  is the molar extinction coefficient of the acceptor and  $f_D$  is the donor fluorescence.  $R_0$  was calculated using  $K^2 = 2/3$  for random orientation (ref 7),  $Q_D = 0.4$ ,  $n = 1.33$ , and  $\epsilon_A(\lambda_{\max}) = 6.5 \times 10^4 \text{ M}^{-1} \text{ cm}^{-1}$ .

(26) Landes, C.; Burda, C.; Braun, M.; El-Sayed, M. A. *J. Phys. Chem. B* **2001**, *105*, 4973–4978.

NL015565N